ORGANIC CHEMISTRY FRONTIERS

CCS 中国化学会 CHINESE CHEMICAL SOCIETY

SIOC 1950

ROYAL SOCIETY OF CHEMISTRY

Is the Polarization of the C=C Bond Imperative for the Bifunctional Outer-Sphere C=C Hydrogenation?

Journal:	*Organic Chemistry Frontiers*
Manuscript ID	QO-RES-12-2022-002020.R1
Article Type:	Research Article
Date Submitted by the Author:	23-Jan-2023
Complete List of Authors:	Ai, Xinliang; Hebei University Xie, Xiaofeng; Hebei University Song, Xue-Qing; Hebei University, College of Pharmaceutical Sciences; Hebei University, College of Pharmaceutical Sciences Li, Longfei; Hebei University, College of Pharmacy Schaefer, Henry; University of Georgia, Computational Chemistry

Is the Polarization of the C=C Bond Imperative for the Bifunctional Outer-Sphere C=C Hydrogenation?

Xinliang Ai,[a+] Xiaofeng Xie,[a+] Xueqing Song,[a] Longfei Li[a]* and Henry F. Schaefer, III[b]*

[a] *College of Pharmacy, Key Laboratory of Pharmaceutical Quality Control of Hebei Province, Key Laboratory of Medicinal Chemistry and Molecular Diagnosis of Ministry of Education, Hebei University, Baoding 071002, Hebei, P. R. China*

[b] *Center for Computational Quantum Chemistry, University of Georgia, Athens, Georgia 30602, United States*

+ *These authors contributed equally to this work.*

*Email: lilongfei@hbu.edu.cn (L.L.); ccq@uga.edu (H.F.S.)

Abstract

Understanding controlling factors is important for the development of the bifunctional outer-sphere C=C hydrogenations. A dominant view is that the polarization of C=C bonds is imperative for these reactions. However, the present comparative DFT study suggests that the polarization of C=C bonds is not the controlling factor. Instead, the "push-pull" type π-conjugative effect can decrease activation barriers and contribute to the outer-sphere bifunctional C=C bond hydrogenations. What is more, this study shows the feasibility of the asymmetric bifunctional outer-sphere C=C hydrogenation.

1. Introduction

Transition-metal-catalyzed alkene hydrogenation is one of the most impactful reactions, and widely applied in the pharmaceutical, agrochemical, and commodity chemical industries.[1] Much of alkene hydrogenations rely on single-site precious metal catalysts involving formal metal ±2 redox steps, such as Wilkinson's catalyst[2], the Schrock-Osborn catalyst[3], and Crabtree's catalyst[4]. The alkene substrates coordinate with metals, and the activations of C=C bonds can be controlled by the d→π* back-bonding interactions according to Dewar-Chatt model.[5] Due to the high cost, toxicity, and potential depletion of precious metals, increased focus has been given to developing catalysts using earth-abundant first-row transition metals.[6] The challenge is the propensity of the late 3d metals to undergo single-electron processes,[7] and several strategies have been proposed to overcome this issue.[8] Hanson reported a Co catalyst featuring a reactive pincer ligand for catalytic alkene hydrogenations, and proposed a nonbifunctional inner-sphere alkene hydrogenation mechanism, as shown in Scheme 1a.[9]

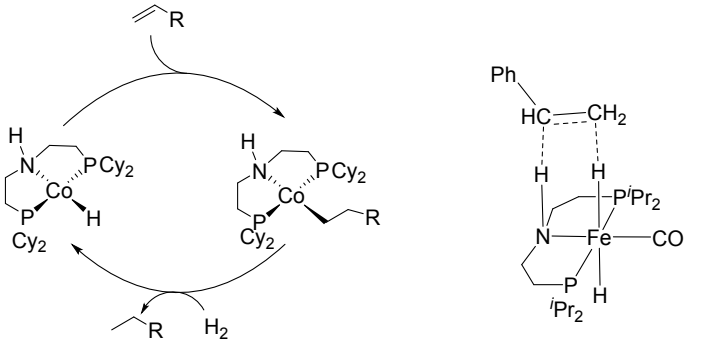

Nonbifunctional Inner-Sphere C=C Hydrogenation (a)

Bifunctional Outer-Sphere C=C Hydrogenation (b)

Scheme 1. The nonbifunctional inner-sphere and bifunctional outer-sphere mechanisms for alkene hydrogenations by metal pincer complexes.

In 2016, Jones and coworkers reported bifunctional stepwise outer-sphere hydrogenations of various styrene derivates with the Fe pincer catalyst ($PNHP^{iPr}$)$Fe(H)_2(CO)$ (Scheme 1b),[10] and the Fe center remains the +2 oxidation state in the catalytic cycle. This state-of-the-art C=C bond hydrogenation process took a great step toward earth-abundant metals facilitated alkene hydrogenations, and has attracted wide attentions.[6c, 11] What is more, Jones and coworkers proposed that the polarization of C=C bonds was imperative for the stepwise outer-sphere C=C hydrogenation process. Nevertheless, the atomic charges of carbons in the compared C=C bonds are not clear, and the activation barriers in non-polar solvent benzene ($\varepsilon = 2.27$) were reported to be less than those in the polar solvent THF ($\varepsilon = 7.43$). Although the bifunctional outer-sphere mechanism is well established in the hydrogenations of polar C=O and C=N bonds,[12] the effect of C=C bond polarization on the outer-sphere C=C hydrogenation is worth reconsidering.

Shedding light on the controlling factor for the bifunctional outer-sphere C=C bond hydrogenation will also be important for developing new alkene hydrogenation reactions based on earth-abundant metals, especially the asymmetric alkene hydrogenations. In this work, we theoretically investigate the metal catalyzed bifunctional outer-sphere C=C hydrogenations to provide clear answers to the above-noted questions.

2. Computational Methods

In accordance with our previous theoretical studies on homogeneous catalytic reactions,[13] all computations in this study were carried out by the DFT method with the ωB97X-D[14] functional using the Gaussian 09 program.[15] Geometries were optimized in toluene solution using the BS-I basis sets, where the 6-311+G(d, p) basis sets were used for nonmetal atoms, and the SDD basis sets with effective core potentials were used for Mn.[16] The single-point energy refinements were further performed with the BS-II basis sets, where the 6-311++G(2df, 2pd) basis sets were used for nonmetal atoms, and the SDD basis sets with effective core potentials were used for Mn atoms.[17] Thermal corrections and entropy contribution to the Gibbs free energies were obtained with the ωB97X-D/BS-I method. The solvent effect was evaluated using the SMD (solution model based on density) solvation model.[18] Harmonic frequency analysis was performed to verify the optimized geometries to be minima (no imaginary frequency) or transition states (TSs, having unique one imaginary frequency). All transition states were verified by employing the intrinsic reaction coordinate (IRC) procedure.[19] Natural bond orbital (NBO) analyses were performed using the NBO 7.0 program.[20] The Cartesian coordinates of all optimized structures are presented in the Supporting Information.

3. Results and Discussion

The effects of the C=C bond polarization are first evaluated. As shown in Figure 1, the alkene substrates are modulated by varying the substituents, and the phenyl derived

substituents (-Ph-OCH_3, -Ph, -Ph-NO_2) were introduced in Jones's work.[10] Partial atomic charges provide the most widely used model for molecular polarization, and have been used to measure the polarity of double bonds by Truhlar et al.[21] The partial atomic charge differences (ACD) between two carbons in C(1)=C(2) bonds are computed via the Natural Bond Orbital (NBO) method[22] to measure the degree of bond polarization. The C(2) atoms adjacent to the substituents are suggested to be more positive than the C(1) atoms. The Mn pincer complex **A1**, which can medicate the hydrogenation of C=C bond in enone molecules,[23] is selected as the catalyst model. The entire pathways for catalytic bifunctional alkene hydrogenations by the Mn pincer complex are shown in Figure S1 in the SI, and two pathways over the transition state **TS1** or **TS2** exist for the hydride transfer as shown in Figure 1. As for the optimized geometric structures of **TS1** and **TS2** (Figure 2), the N-H bond lengths are elongated slightly (within 0.06 Å), but the Mn-H bond lengths are significantly elongated by ca. 0.2 Å compared by the pincer complex **A1**. Therefore, the structures of both **TS1** and **TS2** are in close proximity to a hydride transferring transition state. After the hydride transfer, the amine proton will transfer to the other carbon atom spontaneously without a transition state or require another transition state. The controlling factor for the stepwise or concerted bifunctional hydrogenation mechanism is described in Figure S1 in the SI. The hydride transfer step is rate-determining in the outer-sphere bifunctional hydride/hydrogen addition processes, and will be compared as described in Figure 3.

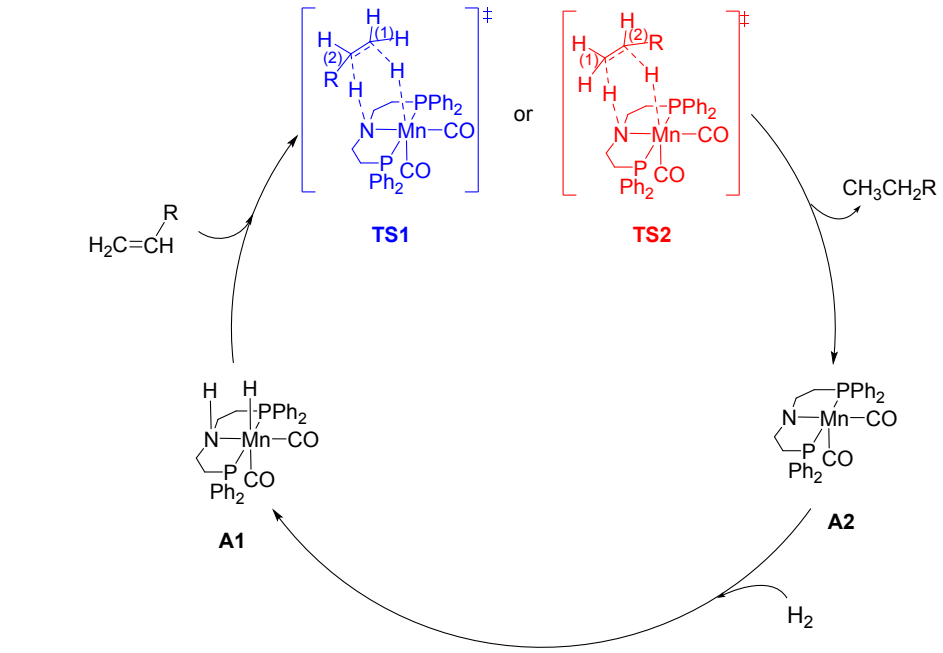

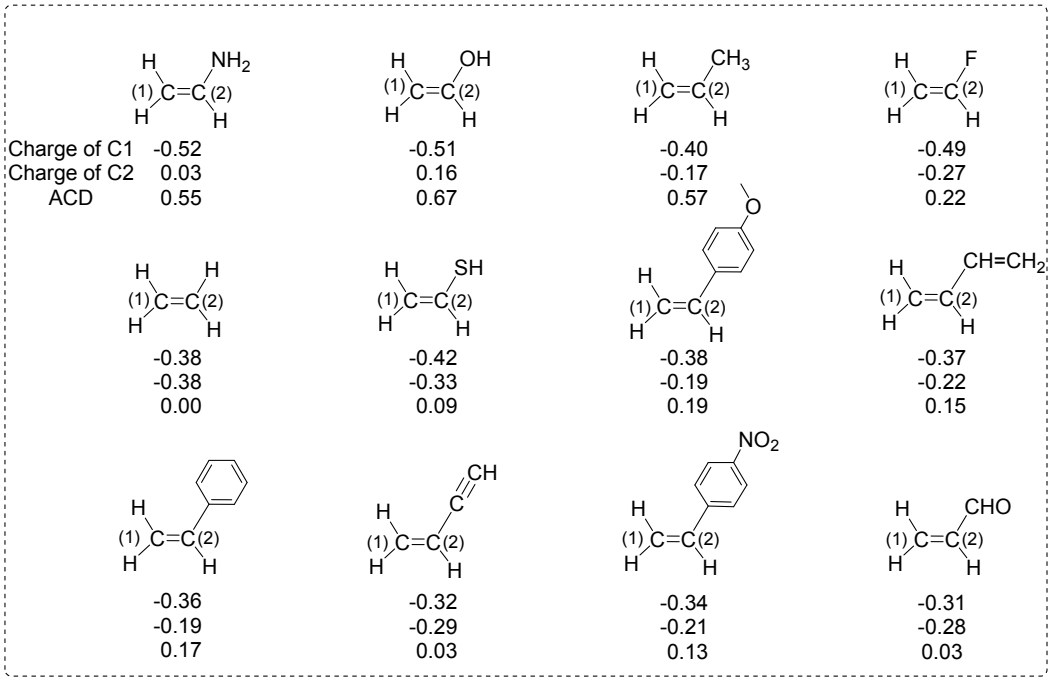

Figure 1. The selected Mn pincer catalyst model and alkene models for the catalytic bifunctional outer-sphere C=C bond hydrogenations. ACD stands for the partial atomic charge difference between two carbons in C=C bonds.

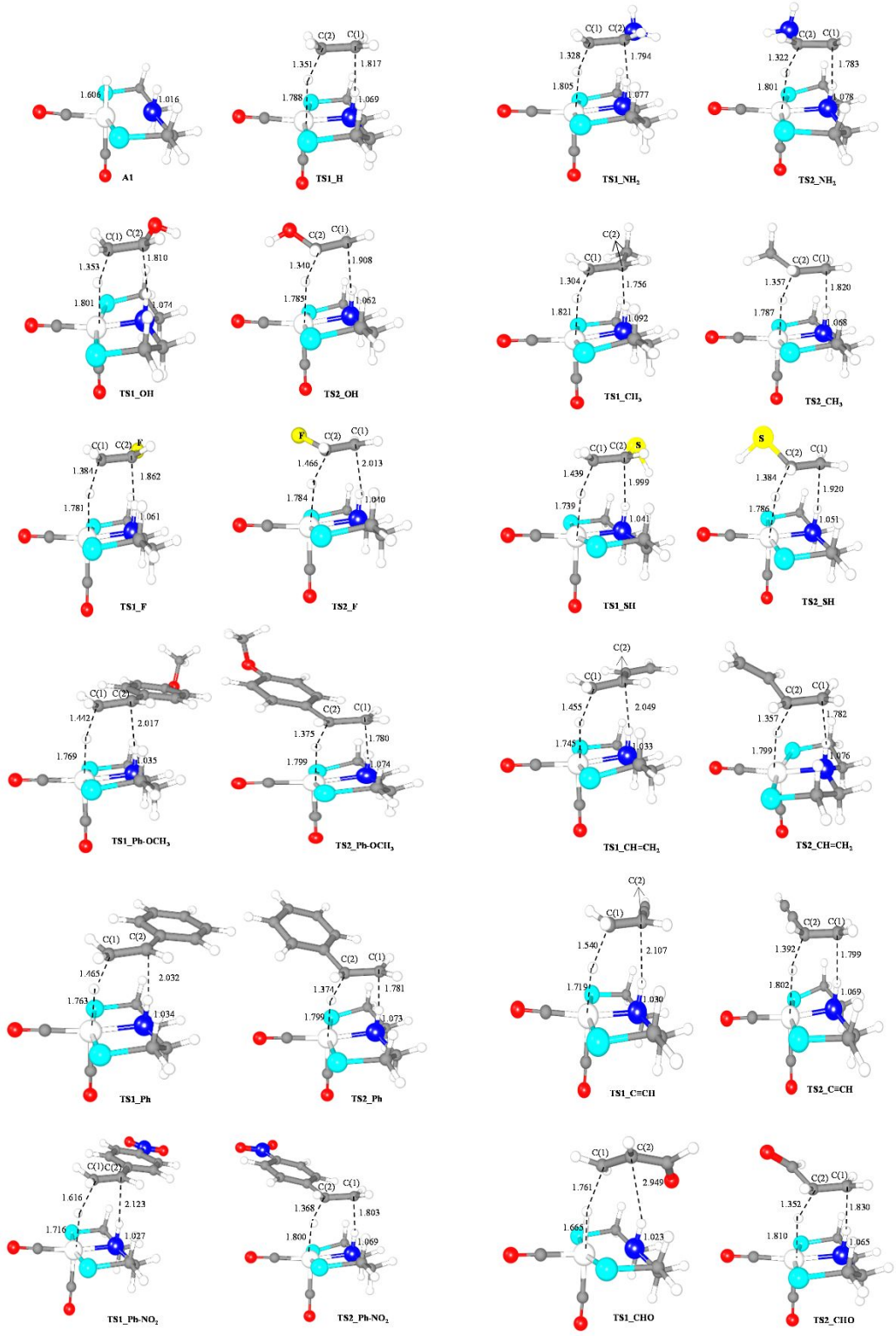

Figure 2. The optimized geometric structures of transition states **TS1** and **TS2**. The benzene groups on the phosphine ligands of Mn compounds are omitted for clarity, and distances are in Å.

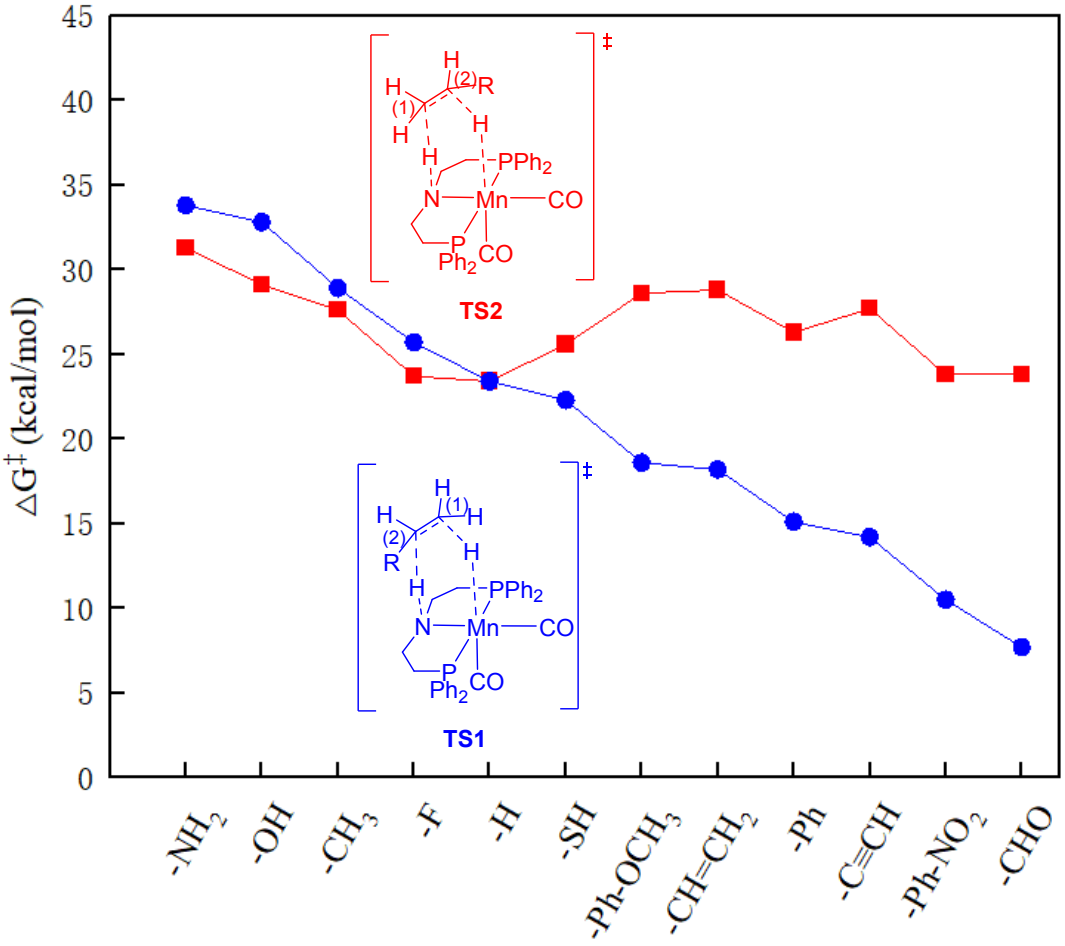

Figure 3. The Gibbs free energy barriers ($\Delta G^{\ddagger}$ in kcal/mol) for the transition states **TS1** (blue line) and **TS2** (red line).

The nonpolar ethylene molecule is selected as the reference, and predicted to own a Gibbs free energy barrier ($\Delta G^{\ddagger}$) of 23.4 kcal/mol for the transition state **TS1** (or **TS2**). For the alkene derivates with -NH_2, -OH, -CH_3 and -F substituents, the energy barriers for **TS2** are lower than those of **TS1**, suggesting that the hydride in **A1** prefers attacking the more positive internal C(2) atom in the C(1)=C(2) bonds. This agrees with the fact that the hydride attacks the positive carbonylic carbon atom in bifunctional C=O

hydrogenations. However, the polarization of C=C bonds does not decrease the energy barriers compared with the nonpolar ethylene molecule. The -CH_3 and -F substituents can induce the C=C bond polarization with ACD being 0.23 e, but the corresponding $\Delta G^{\ddagger}$ values of **TS2** increase to 23.7~27.6 kcal/mol. When C=C bonds are further polarized by the -NH_2 and -OH substituents (0.55 and 0.67 e for ACD), the corresponding $\Delta G^{\ddagger}$ values of **TS2** increase to 29.1~31.3 kcal/mol. Therefore, the polarization of C=C bonds could not be the controlling factor for the outer-sphere bifunctional C=C bond hydrogenations.

Next we turn to the alkene derivates with conjugated -SH, -Ph-OCH_3, -$CH{=}CH_2$, -Ph, -C≡CH, -Ph-NO_2 and -CHO substituents, and their C=C bonds are polarized a little with low ACD values (within 0.2 e). Interestingly, the blue line falls below the red line on the right side of Figure 2, and suggests the negative hydride ligand in **A1** prefers attacking the negative terminal C(1) atoms via **TS1** rather than the positive C(2) atoms via **TS2**. This provides robust evidence that the polarization of C=C bonds is not the controlling factor for the outer-sphere bifunctional C=C bond hydrogenations. Since the energy barriers of **TS1** can be decreased by these conjugated substituents, the facile bifunctional outer-sphere C=C hydrogenation could be achieved, and the factors determining the energy barriers of **TS1** are investigated as shown below.

The energy barriers of transition states **TS1** could be controlled by the "push-pull" effect which is a nickname for describing the enhancement of π-conjugation in the donor-

(π-linker)-acceptor compounds where the electron-donating and the electron-accepting moieties are linked by a conjugate system.[24] The "push-pull" strategy has been reported to be effective in stabilizing unstable intermediates by us[25] and transition states by Herrera et al[26]. Recently, the "push-pull" strategy has been used in stabilizing solar cells.[27] For the transition state **TS1**, the electron-withdrawing substituents (e.g. -CHO) provide the "pull" effects, and the moving hydrides provide the "push" effects as shown in Figure 4a. As a result, such "push-pull" effects will strengthen the π-conjugations between C=C bonds and substituents of alkene derivative moieties in **TS1**, and the length of C(2)-C(3) bond decreases from 1.540 Å in free enone molecule to 1.432 Å in **TS1**. Therefore, transition state **TS1** is stabilized by "push-pull" effect with leading to low energy barriers. In contrast, the electron-donating substituents (e.g. -NH_2) provide the "push" effects as shown in Figure 4b, and the resulting "push-push" effects will weaken the π-conjugations between C=C bonds and substituents of alkene derivative moieties in **TS1**. The length of C(2)-N bond increases from 1.384 Å in free ethenamine molecule to 1.448 Å in **TS1**. Therefore, transition state **TS1** is destabilized by "push-push" effect with leading to high energy barriers.

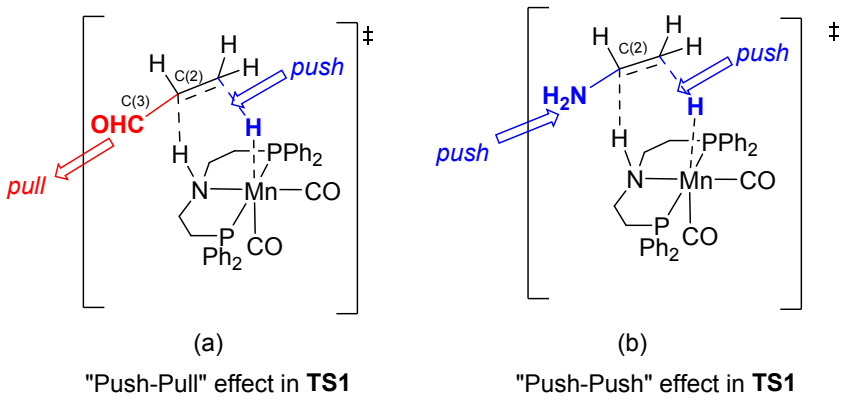

Figure 4. The "push-pull" and "push-push" effects present in the transition states **TS1**.

The red and blue lines in Figure 3 become separated after the dot for ethylene, which could also be accounted by the "push-pull" effects. The π-conjugative stabilization effect between C=C bond and substituent does not exist when the hydride moves to the internal C(2) atom through **TS2**, in which the N-H bond is not elongated significantly and the amine proton is far from the substrate. As a result, the alkene derivatives with -NH_2 or -OH have low π-conjugative stabilizations in both **TS1** and **TS2**, and the differences of $\Delta G^{\ddagger}$ values are small with the red dots being near to the blue dots in Figure 3. In contrast, the alkene derivate with the -CHO substituent displays high π-conjugative stabilization in **TS1** but low π-conjugative stabilization in **TS2**; therefore, the differences of $\Delta G^{\ddagger}$ values are large with the red dots being far from the blue dots in Figure 3.

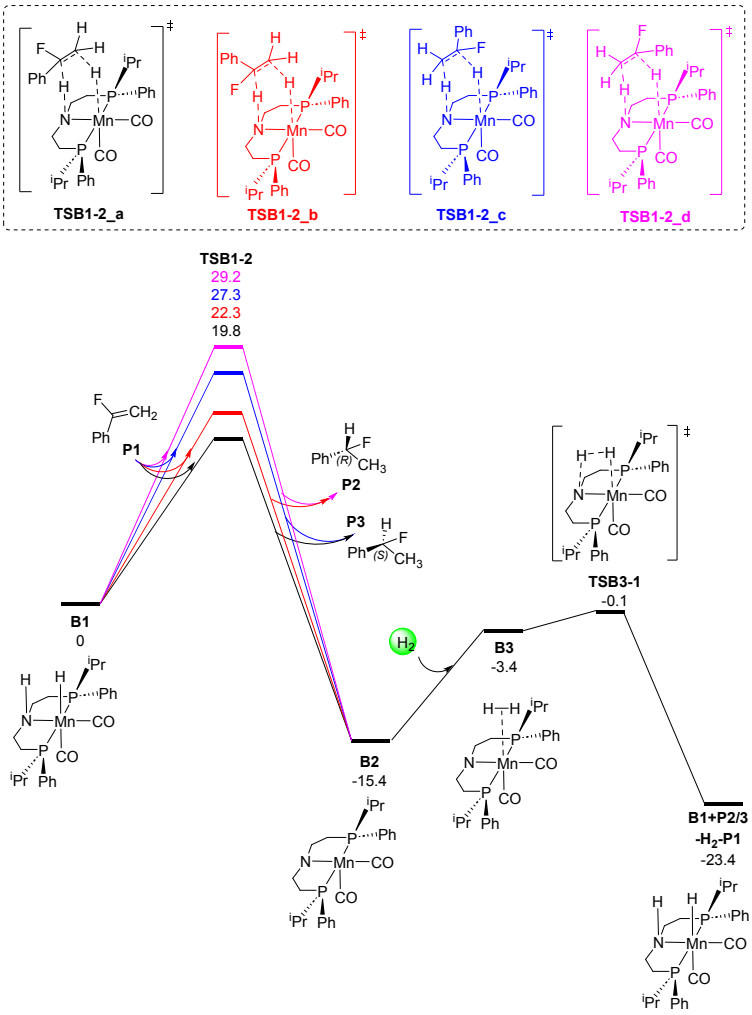

Figure 5. The energy profiles for the designed asymmetric outer-sphere bifunctional C=C bond hydrogenations catalyzed by the chiral Mn pincer complex **B1**. The relative Gibbs free energies (ΔG) are in kcal/mol.

The metal facilitated asymmetric bifunctional outer-sphere bifunctional C=O hydrogenations have been well established, such as the Noyori type catalysts.[28] To our knowledge, the metal catalyzed asymmetric outer-sphere bifunctional C=C hydrogenations have not been reported. Since the DFT method has been widely used in designing asymmetric catalytic reactions,[29] we explore the possibility of this reaction. The new Mn pincer catalyst **B1** featuring stereogenic phosphorous centers is adopted, and the prochiral

(1-fluorovinyl)benzene is selected as substrate model (Figure 5). Through the concerted outer-sphere bifunctional hydride/hydrogen transfer, the C=C bonds are reduced with forming two stereoisomeric products, and four possible transition states exist for the process. The generated **B2** undergoes the hydrogen addition to regenerate the starting species **B1** through the transition state **TSB3-1** with an energy barrier of 15.3 kcal/mol. The chiral-determining transition state **TSB1-2_a** has a Gibbs free energy barrier of 19.8 kcal/mol, which is 2.5 kcal/mol ($\Delta\Delta G^{\ddagger}$) lower than that of the second-lowest transition state **TSB1-2_b**. According to the computed $\Delta G^{\ddagger}$ and $\Delta\Delta G^{\ddagger}$ values, the designed asymmetric outer-sphere bifunctional C=C bond hydrogenations could have both high activities and enantioselectivities. This study is the first to report the asymmetric outer-sphere bifunctional C=C bond hydrogenation, and lays out a much-needed mechanistic foundation that should guide the continuing development of these reactions in the industry and academic research.

Conclusions

A comparative study is performed on Mn pincer complex facilitated alkene hydrogenations, and suggests that the polarization of C=C bonds is not the controlling factor for the outer-sphere bifunctional C=C bond hydrogenations. Further, it is suggested the "push-pull" π-conjugative stabilization effect can contribute to outer-sphere bifunctional C=C bond hydrogenations by decreasing the activation barriers of **TS1**, but

the "push-push" effects disfavor the process with increasing activation barriers. Asymmetric outer-sphere bifunctional C=C bond hydrogenations catalyzed by the chiral pincer complex **B1** are further designed, and predicted to have both high activities and enantioselectivities.

ASSOCIATED CONTENT

Supporting Information

Optimized geometries and energies of all stationary points along the reaction pathways, the imaginary vibrational frequencies of transition states (PDF)

Notes

The authors declare no competing financial interest.

Acknowledgments

This work was supported by the National Natural Science Foundation of China (No. 21903018), the Natural Science Interdisciplinary Research Program of Hebei University (No. DXK202013), the Natural Science Foundation of Hebei Province (B2021201019) and the Innovation Capacity Improvement Plan of Hebei Province (Grant No. 20567605H). We thank the High Performance Computer Center of Hebei University for providing computational resources. HFS was supported by the U.S. Department of Energy, Basic Energy Sciences, Division of Chemistry, Computational and Theoretical Chemistry (CTC) program, Contract No. DE-SC0018412.

Reference

1 L. Massaro, J. Zheng, C. Margarita and P. G. Andersson, Enantioconvergent and enantiodivergent catalytic hydrogenation of isomeric olefins, *Chem. Soc. Rev.*, 2020, **49**, 2504-2522.

2 J. A. Osborn, F. H. Jardine, J. F. Young and G. Wilkinson, The preparation and properties of tris(triphenylphosphine)halogenorhodium(I) and some reactions thereof including catalytic homogeneous hydrogenation of olefins and acetylenes and their derivatives, *J. Chem. Soc. (A)*, 1966, **0**, 1711–1732.

3 R. R. Schrock and J. A. Osborn, Catalytic Hydrogenation Using Cationic Rhodium Complexes. I. Evolution of the Catalytic System and the Hydrogenation of Olefins, *J. Am. Chem. Soc.*, 1976, **98**, 2134–2143.

4 R. H. Crabtree, Iridium Compounds in Catalysis, *Acc. Chem. Res.*, 1979, **12**, 331-337.

5 (a) J. Chatt and L. A. Duncanson, 586. Olefin co-ordination compounds. Part III. Infra-red spectra and structure: attempted preparation of acetylene complexes, *J. Chem. Soc.*, 1953, 2939-2947; (b) C. Wentrup, Zeise, Liebig, Jensen, Huckel, Dewar, and the Olefin pi-Complex Bonds, *Angew. Chem. Int. Ed.*, 2020, **59**, 8332-8342.

6 (a) G. A. Filonenko, R. van Putten, E. J. M. Hensen and E. A. Pidko, Catalytic (de)hydrogenation promoted by non-precious metals - Co, Fe and Mn: recent advances in an emerging field, *Chem. Soc. Rev.*, 2018, **47**, 1459-1483; (b) L. Alig, M. Fritz and S. Schneider, First-Row Transition Metal (De)Hydrogenation Catalysis Based On Functional Pincer Ligands, *Chem. Rev.*, 2019, **119**, 2681-2751; (c) S. W. Anferov, A. S. Filatov and J. S. Anderson, Cobalt-Catalyzed Hydrogenation Reactions Enabled by Ligand-Based Storage of Dihydrogen, *ACS Catal.*, 2022, **12**, 9933-9943.

7 W. H. Harman and J. C. Peters, Reversible H_2 addition across a nickel-borane unit as a promising strategy for catalysis, *J. Am. Chem. Soc.*, 2012, **134**, 5080−5082.

8 W. Taniguchi, J.-i. Ito and M. Yamashita, CNC-pincer iron complexes containing a bis(N-heterocyclic carbene)Amido ligand: Synthesis and application to catalytic hydrogenation of alkenes, *J. Organomet. Chem.*, 2020, **923**, 121436.

9 (a) K. V. Vasudevan, B. L. Scott and S. K. Hanson, Alkene Hydrogenation Catalyzed by Nickel Hydride Complexes of an Aliphatic PNP Pincer Ligand, *Eur. J. Inorg. Chem.*, 2012, 4898-4906; (b) G. Zhang, B. L. Scott and S. K. Hanson, Mild and homogeneous cobalt-catalyzed hydrogenation of C=C, C=O, and C=N bonds, *Angew. Chem. Int. Ed.*, 2012, **51**, 12102 –12106; (c) T. P. Lin and J. C. Peters, Boryl-mediated reversible H_2 activation at cobalt: catalytic hydrogenation, dehydrogenation, and transfer hydrogenation, *J. Am. Chem. Soc.*, 2013, **135**, 15310-15313; (d) G. Zhang, Z. Yin and J. Tan, Cobalt(ii)-catalysed transfer hydrogenation of olefins, *RSC Adv.*, 2016, **6**, 22419-22423.

10 R. Xu, S. Chakraborty, S. M. Bellows, H. Yuan, T. R. Cundari and W. D. Jones, Iron-Catalyzed Homogeneous Hydrogenation of Alkenes under Mild Conditions by a Stepwise, Bifunctional Mechanism, *ACS Catal.*, 2016, **6**, 2127-2135.

11 (a) M. K, Karunananda and N. P. Mankad, Cooperative Strategies for Catalytic Hydrogenation of Unsaturated Hydrocarbons, *ACS Catal.*, 2017, **7**, 6110-6119; (b) J. Chen, J. Guo and Z. Lu, Recent

Advances in Hydrometallation of Alkenes and Alkynes via the First Row Transition Metal Catalysis, *Chin. J. Chem.*, 2018, **36**, 1075-1109; (c) M. Espinal-Viguri, S. E. Neale, N. T. Coles, S. A. Macgregor and R. L. Webster, Room Temperature Iron-Catalyzed Transfer Hydrogenation and Regioselective Deuteration of Carbon-Carbon Double Bonds, *J. Am. Chem. Soc.*, 2019, **141**, 572-582; (d) S. Weber, B. Stöger, L. F. Veiros and K. Kirchner, Rethinking Basic Concepts—Hydrogenation of Alkenes Catalyzed by Bench-Stable Alkyl Mn(I) Complexes, *ACS Catal.*, 2019, **9**, 9715-9720; (e) S. M. W. Rahaman, D. K. Pandey, O. Rivada-Wheelaghan, A. Dubey, R. R. Fayzullin and J. R. Khusnutdinova, Hydrogenation of Alkenes Catalyzed by a Non‐pincer Mn Complex, *ChemCatChem*, 2020, **12**, 5912-5918; (f) M. R. Elsby and R. T. Baker, Strategies and mechanisms of metal-ligand cooperativity in first-row transition metal complex catalysts, *Chem. Soc. Rev.*, 2020, **49**, 8933-8987.

12 O. Eisenstein and R. H. Crabtree, Outer sphere hydrogenation catalysis, *New J. Chem.*, 2013, **37**, 21-27.

13 (a) L. F. Li, M. X. Dong, H. J. Zhu, B. Peng, Y. M. Xie and H. Schaefer, Unusual η^1 -Coordinated Alkyne and Alkene Complexes, *Chem. Eur. J.*, 2019, **25**, 15628-15633; (b) L. Li, Z. Wu, H. Zhu, G. H. Robinson, Y. Xie and H. F. Schaefer, Reduction of Dinitrogen via 2,3'-Bipyridine-Mediated Tetraboration, *J. Am. Chem. Soc.*, 2020, **142**, 6244-6250; (c) C. Liu, L. Zhang, L. Li and M. Lei, Theoretical Design of a Catalyst with Both High Activity and Selectivity in C-H Borylation, *J. Org. Chem.*, 2021, **86**, 16858-16866; (d) X. Zhang, L. Li, Z. Wu, H. Zhu, Y. Xie and H. F. Schaefer, 3rd, Heteroatom (N, P, As, Sb, Bi) Effects on the Resonance-Stabilized 2-, 3-, and 4-Picolyl Radicals, *Inorg. Chem.*, 2021, **60**, 5860-5867; (e) Z. Jia, L. Li, X. Zhang, K. Yang, H. Li, Y. Xie and I. Henry F. Schaefer, Acceleration Effect of Bases on Mn Pincer Complex-Catalyzed CO_2 Hydroboration, *Inorg. Chem.*, 2022, **61**, 3970-3980.

14 J. D. Chai and M. Head-Gordon, Long-range corrected hybrid density functionals with damped atom-atom dispersion corrections, *Phys. Chem. Chem. Phys.*, 2008, **10**, 6615-6620.

15 M. J. Frisch, G. W. Trucks, H. B. Schlegel, G. E. Scuseria, M. A. Robb, J. R. Cheeseman, G. Scalmani, V. Barone, B. Mennucci, G. A. Petersson, H. Nakatsuji, M. Caricato, X. Li, H. P. Hratchian, A. F. Izmaylov, J. Bloino, G. Zheng, J. L. Sonnenberg, M. Hada, M. Ehara, K. Toyota, R. Fukuda, J. Hasegawa, M. Ishida, T. Nakajima, Y. Honda, O. Kitao, H. Nakai, T. Vreven, J. A. Montgomery, Jr. , J. E. Peralta, F. Ogliaro, M. Bearpark, J. J. Heyd, E. Brothers, K. N. Kudin, V. N. Staroverov, R. Kobayashi, J. Normand, K. Raghavachari, A. Rendell, J. C. Burant, S. S. Iyengar, J. Tomasi, M. Cossi, N. Rega, J. M. Millam, M. Klene, J. E. Knox, J. B. Cross, V. Bakken, C. Adamo, J. Jaramillo, R. Gomperts, R. E. Stratmann, O. Yazyev, A. J. Austin, R. Cammi, C. Pomelli, J. W. Ochterski, R. L. Martin, K. Morokuma, V. G. Zakrzewski, G. A. Voth, P. Salvador, J. J. Dannenberg, S. Dapprich, A. D. Daniels, O. Farkas, J. B. Foresman, J. V. Ortiz, J. Cioslowski and D. J. Fox, *Gaussian 09, revision B.01; Gaussian, Inc.: Wallingford, CT,*, 2009.

16 (a) T. Leininger, A. Nicklass, W. Kiichle, H. Stoll, M. Dolg and A. Bergner, The accuracy of the pseudopotential approximation: non-frozen-core effects for spectroscopic constants of alkali fluorides XF (X = K, Rb, Cs), *Chem. Phys. Lett.*, 1996, **255**, 274-280; (b) W. J. Pietro, M. M. Franc, W. J. Hehre, D. J. DeFrees, J. A. Pople and J. S. Binkley, Self-consistent Molecular Orbital Methods. Supplemented Small Split-Valence Basis Sets for Second-Row Elements, *J. Am. Chem. Soc.*, 1982, **104**, 5039-5048.

17 F. Weigend and R. Ahlrichs, Balanced basis sets of split valence, triple zeta valence and quadruple zeta valence quality for H to Rn: Design and assessment of accuracy, *Phys. Chem. Chem. Phys.*, 2005, **7**, 3297-3305.

18 (a) A. V. Marenich, C. J. Cramer and D. G. Truhlar, Universal Solvation Model Based on Solute Electron Density and on a Continuum Model of the Solvent Defined by the Bulk Dielectric Constant and Atomic Surface Tensions, *J. Phys. Chem. B*, 2009, **113**, 6378–6396; (b) J. Tomisi and M. Persico, Molecular Interactions in Solution: An Overview of Methods Based on Continuous Distributions of the Solvent., *Chem. Rev.*, 1994, **7**, 2027-2094.

19 T. Tsutsumi, Y. Ono, Z. Arai and T. Taketsugu, Visualization of the Intrinsic Reaction Coordinate and Global Reaction Route Map by Classical Multidimensional Scaling, *J. Chem. Theory. Comput.*, 2018, **14**, 4263-4270.

20 E. D. Glendening, C. R. Landis and F. Weinhold, NBO 7.0: New vistas in localized and delocalized chemical bonding theory, *J. Comput. Chem.*, 2019, **40**, 2234-2241.

21 R. M. Olson, A. V. Marenich, C. J. Cramer and D. G. Truhlar, Charge Model 4 and Intramolecular Charge Polarization, *J. Chem. Theory Comput.*, 2007, **3**, 2046-2054.

22 S. Achour, Z. Hosni and B. Tangour, Hexene hydrogenation catalysed by the complex monohydrid complexes: A DFT study of associated vs dissociated pathways, *J. Mol. Graph. Model.*, 2020, **98**, 107583.

23 A. Kaithal, M. Holscher and W. Leitner, Carbon monoxide and hydrogen (syngas) as a C1-building block for selective catalytic methylation, *Chem. Sci.*, 2020, **12**, 976-982.

24 (a) E. D. Raczynska, J. F. Gal and P. C. Maria, Enhanced Basicity of Push-Pull Nitrogen Bases in the Gas Phase, *Chem. Rev.*, 2016, **116**, 13454-13511; (b) C. Cao, Z. Zeng and C. Cao, A new insight into the push-pull effect of substituents via the stilbene-like model compounds, *J Phys Org Chem.*, 2022, **35**.

25 L. Li, M. Lei, Y. Xie, H. F. Schaefer, 3rd, B. Chen and R. Hoffmann, Stabilizing a different cyclooctatetraene stereoisomer, *Proc. Natl. Acad. Sci. U. S. A.*, 2017, **114**, 9803-9808.

26 J. V. Alegre-Requena, E. Marqués-López and R. P. Herrera, "Push–Pull π+/π–" (PPππ) Systems in Catalysis, *ACS Catal.*, 2017, **7**, 6430-6439.

27 (a) Y. Hu, A. Alsaleh, O. Trinh, F. D'Souza and H. Wang, β-Functionalized push–pull opp-dibenzoporphyrins as sensitizers for dye-sensitized solar cells: the push group effect, *J. Mater. Chem. A*, 2021, **9**, 27692-27700; (b) M. P. Aplan, Y. Lee, C. A. Wilkie, Q. Wang and E. D. Gomez, Push–pull architecture eliminates chain length effects on exciton dissociation, *J. Mater. Chem. A*, 2018, **6**, 22758-22767; (c) D. Bansal, A. Kundu, V. P. Singh, A. K. Pal, A. Datta, J. Dasgupta and P. Mukhopadhyay, A highly contorted push-pull naphthalenediimide dimer and evidence of intramolecular singlet exciton fission, *Chem. Sci.*, 2022, **13**, 11506-11512; (d) M. Ito, M. Sakai, N. Ando and S. Yamaguchi, Electron-Deficient Heteroacenes that Contain Two Boron Atoms: Near-Infrared Fluorescence Based on a Push-Pull Effect, *Angew. Chem. Int. Ed. Engl.*, 2021, **60**, 21853-21859.

28 (a) W. S. Knowles and R. Noyori, Pioneering Perspectives on Asymmetric Hydrogenation, *Acc. Chem. Res.*, 2007, **40**, 1238-1239; (b) R. H. Morris, Exploiting metal-ligand bifunctional reactions in the design

of iron asymmetric hydrogenation catalysts, *Acc. Chem. Res.*, 2015, **48**, 1494-1502; (c) M. Garbe, K. Junge, S. Walker, Z. Wei, H. Jiao, A. Spannenberg, S. Bachmann, M. Scalone and M. Beller, Manganese(I)-Catalyzed Enantioselective Hydrogenation of Ketones Using a Defined Chiral PNP Pincer Ligand, *Angew. Chem. Int. Ed.*, 2017, **56**, 11237-11241; (d) P. A. Dub and J. C. Gordon, The role of the metal-bound N–H functionality in Noyori-type molecular catalysts, *Nat. Rev. Chem.*, 2018, **2**, 396-408; (e) M. Garbe, Z. Wei, B. Tannert, A. Spannenberg, H. Jiao, S. Bachmann, M. Scalone, K. Junge and M. Beller, Enantioselective Hydrogenation of Ketones using Different Metal Complexes with a Chiral PNP Pincer Ligand, *Adv. Synth. Catal.*, 2019, **361**, 1913-1920.

29 (a) K. N. Houk and P. H. Cheong, Computational prediction of small-molecule catalysts, *Nature*, 2008, **455**, 309-313; (b) K. H. Hopmann, Quantum chemical studies of asymmetric reactions: Historical aspects and recent examples, *Int. J. Quantum Chem.*, 2015, **115**, 1232-1249; (c) A. C. Doney, B. J. Rooks, T. Lu and S. E. Wheeler, Design of Organocatalysts for Asymmetric Propargylations through Computational Screening, *ACS Catal.*, 2016, **6**, 7948-7955; (d) Y. Guan and S. E. Wheeler, Automated Quantum Mechanical Predictions of Enantioselectivity in a Rhodium-Catalyzed Asymmetric Hydrogenation, *Angew. Chem. Int. Ed.*, 2017, **56**, 9101-9105; (e) O. Alioui, M. Badawi, A. Erto, M. A. Amin, V. Tirth, B.-H. Jeon, S. Islam, M. Balsamo, M. Virginie, B. Ernst and Y. Benguerba, Contribution of DFT to the optimization of Ni-based catalysts for dry reforming of methane: a review, *Catal. Rev.*, 2022, 1-53.